IOPscience iopscience.iop.org

Home Search Collections Journals About Contact us My IOPscience

Universal features of the shapes of percolation clusters and lattice animals

This article has been downloaded from IOPscience. Please scroll down to see the full text article.

1987 J. Phys. A: Math. Gen. 20 2539

(http://iopscience.iop.org/0305-4470/20/9/038)

View the table of contents for this issue, or go to the journal homepage for more

Download details:
IP Address: 129.252.86.83
The article was downloaded on 31/05/2010 at 12:19

Please note that terms and conditions apply.

J. Phys. A: Math. Gen. **20** (1987) 2539-2556. Printed in the UK

Universal features of the shapes of percolation clusters and lattice animals

Joseph A Aronovitz†‡ and Michael J Stephen§

† Lyman Laboratory of Physics, Harvard University, Cambridge, MA 02138, USA
§ Physics Department, Rutgers University, New Brunswick, NJ 08903, USA

Received 12 August 1986

Abstract. The shapes of percolation clusters and lattice animals are investigated. The universal quantities Δ_d and S_d, which were introduced to measure the average asymmetry and degree of prolate- or oblateness, respectively, of long-chain polymers, are here computed in an ε expansion for percolation clusters and for lattice animals. Δ_d is computed to $O(\varepsilon)$, while S_d is computed to $O(1)$. The clusters are shown to be on average anisotropic and prolate, but less so than polymers. Percolation clusters and lattice animals have identical shapes above eight dimensions. Below $d = 8$ animals are slightly more anisotropic than percolation clusters.

1. Introduction

The properties of clusters in percolation-type lattice models have long been of physical interest [1]. For instance, percolation models describe the connectivities of random networks and are connected with phase transitions in magnetic systems with quenched positional disorder. Lattice animals are closely related to dilute solutions of branch polymers in good solvents [2]. Most investigations into such models to date have been directed towards computing average cluster sizes and densities. The question of cluster shapes has remained open.

Recently, Family *et al* [3] used numerical techniques to investigate the shapes, in two dimensions, of bond and growing bond percolation clusters at the percolation threshold p_c, and of lattice animals. They found in all three cases that the average cluster is quite asymmetric in the limit of large clusters. At first, this result seems to be surprising. After all, the underlying ensembles of all three models are isotropic. However, isotropy of an ensemble only implies that a given cluster conformation will appear with equal probability in arbitrary orientations. The degree of anisotropy of a typical conformation is a question of phase space, rather than of the symmetry of the ensemble.

The observed anisotropy of clusters is quite similar to that computed for long-chain polymers in dilute solutions of either good or theta solvents. Over the last fifteen years, asymmetries in polymer shapes have been investigated in a number of Monte Carlo studies [4-9]. Recently, analytic progress has also been made. In the last year parameters describing polymer shapes have been computed in mean-field theory [10], in an expansion in the inverse spatial dimension $1/d$ [11] and in an ε expansion [12].

‡ Present address: Department of Physics, University of Pennsylvania, Philadelphia, PA 19104, USA.

0305-4470/87/092539+18$02.50 © 1987 IOP Publishing Ltd

The $1/d$ expansion takes advantage of the fact that for $d=\infty$ there is really only one random walk of finite length, while the other calculations were made possible by characterising the polymer shapes in terms of analytically computable parameters.

In this paper we apply Aronovitz and Nelson's [12] characterisations of shape, Δ_d† and S_d to both bond percolation and to lattice animals. We compute these quantities at p_c because they are universal there. Our results show that both models have inherent anisotropy and that lattice animals are slightly more anisotropic than percolation clusters. In § 2 we describe how Δ_d and S_d characterise shapes and adapt these measures to clusters. We prove rigorous bounds on Δ_d and S_d in d dimensions in appendix 1. In § 3, we use the connection between bond percolation and the n-state Potts model in the $n\to 1$ limit [13] to compute Δ_d in an $\varepsilon=6-d$ expansion to $O(\varepsilon)$, and to compute S_d to $O(1)$. In § 4, we use a similar connection between lattice animals and the $n\to 0$ limit of a modified Potts model [14] to extend the calculation of § 3 to the lattice animal case, now in an $\varepsilon=8-d$ expansion. Finally, in § 5 we discuss our results and compare them to corresponding results on the shapes of polymers.

2. Characterising cluster shapes

In order to study cluster shapes, we must first define quantities which measure the shape of the average cluster and are computable. Suppose that the shape of a given cluster G is characterised by a symmetric, positive definite tensor $\boldsymbol{Q}(G)$, for example the moment of inertia, having eigenvalues $\lambda_1 \geqslant \ldots \geqslant \lambda_d$. If all the λ_i are equal, G is spherically symmetric. Otherwise, we can probe the anisotropy of G by studying variations in the λ_i.

Family *et al* [3] choose to define an asymmetry measure $A(G)=\lambda_d/\lambda_1$. A satisfies

$$0 \leqslant A \leqslant 1 \tag{2.1}$$

with $A(G)=1$ corresponding to spherical symmetry. They numerically average A over ensembles of two-dimensional clusters containing N sites, and in the limit $N\to\infty$ in two dimensions find that

$$A_2^{\text{animals}} \simeq 0.29 \tag{2.2a}$$

$$A_2^{\text{percolation}} \simeq 0.4. \tag{2.2b}$$

These results show that both animals and percolation clusters are, on average, anisotropic, the animals slightly more so.

Unfortunately, A is quite difficult to treat analytically. Computing averages of specific eigenvalues would require diagonalising a $d\times d$ matrix of fields explicitly and then averaging the resulting expression. A more tractable approach is that used by Aronovitz and Nelson to study polymer shapes. They characterise the shapes using ratios of rotationally invariant polynomials of Q_{ij}. Averages of such polynomials become Green functions upon mapping the problem onto a field theory. Their ratios can then be computed in an ε expansion.

Let the average eigenvalue of $\boldsymbol{Q}$ be

$$\bar{\lambda} \equiv \frac{1}{d}\sum_i \lambda_i = \frac{1}{d}\,\mathrm{Tr}\,\boldsymbol{Q}. \tag{2.3}$$

† Rudnick and Gaspari [10] compute Δ_d for polymers (called A_d) in mean-field theory.

It is convenient to define $\hat{\boldsymbol{Q}}$, the traceless version of $\boldsymbol{Q}$:

$$\hat{\boldsymbol{Q}} = \boldsymbol{Q} - \bar{\lambda}\mathbf{1}. \tag{2.4}$$

If G were spherical, then $\hat{\boldsymbol{Q}}$ would be $\mathbf{0}$. The relative eigenvalue variance

$$\sum_i \left(\frac{\lambda_i - \bar{\lambda}}{\bar{\lambda}}\right)^2 = d^2 \frac{\operatorname{Tr} \hat{\boldsymbol{Q}}^2}{(\operatorname{Tr} \boldsymbol{Q})^2}$$

is a measure of the anisotropy of G. We prove in appendix 1 that for each cluster G

$$0 \leqslant \frac{d}{d-1} \operatorname{Tr} \hat{\boldsymbol{Q}}^2(G) \leqslant (\operatorname{Tr} \boldsymbol{Q}(G))^2. \tag{2.5}$$

Upon averaging, (2.5) leads to the exact inequality

$$0 \leqslant \Delta_d \equiv \frac{d}{d-1} \frac{\langle \operatorname{Tr} \hat{\boldsymbol{Q}}^2 \rangle}{\langle (\operatorname{Tr} \boldsymbol{Q})^2 \rangle} \leqslant 1. \tag{2.6}$$

We choose Δ_d as a normalised measure of anisotropy.

The character of the anisotropy of G is reflected by $T(G) = \operatorname{Tr} \hat{\boldsymbol{Q}}^3$. In three dimensions,

$$\operatorname{Tr} \hat{\boldsymbol{Q}}^3 = 3 \det \hat{\boldsymbol{Q}} = 3(\lambda_1 - \bar{\lambda})(\lambda_2 - \bar{\lambda})(\lambda_3 - \bar{\lambda})$$

so that T is positive when G is prolate and is negative when G is oblate. We show in appendix 1 that, even in higher dimensions, the sign of T still reflects the relative number of large and small eigenvalues in $\boldsymbol{Q}$. We also prove that

$$-\frac{(\operatorname{Tr} \boldsymbol{Q})^3}{(d-1)^3} \leqslant \frac{d^2}{(d-1)(d-2)} \operatorname{Tr} \hat{\boldsymbol{Q}}^3 \leqslant (\operatorname{Tr} \boldsymbol{Q})^3. \tag{2.7}$$

Upon averaging, (2.7) proves that S_d†, our normalised measure of the character of cluster anisotropy, satisfies

$$-\frac{1}{(d-1)^3} \leqslant S_d \equiv \frac{d^2}{(d-1)(d-2)} \frac{\langle \operatorname{Tr} \hat{\boldsymbol{Q}}^3 \rangle}{\langle (\operatorname{Tr} \boldsymbol{Q})^3 \rangle} \leqslant 1. \tag{2.8}$$

In order to completely specify Δ_d and S_d, we still must define the shape tensor $\boldsymbol{Q}(G)$. Suppose G is a connected cluster of bonds on a lattice whose αth site is located at $\boldsymbol{r}^\alpha$. Further assume that the origin is connected to G, and define

$$C^{(m+1)}_{\alpha_1 \ldots \alpha_m}(G) = \begin{cases} 1 & \text{if the sites } \alpha_1, \ldots, \alpha_m \text{ are connected to } G \\ 0 & \text{otherwise.} \end{cases} \tag{2.9}$$

Notice that the $C^{(m)}$ have the factorisation property

$$C^{(m+1)}_{\alpha_1 \ldots \alpha_m}(G) = C^{(2)}_{\alpha_1}(G) C^{(2)}_{\alpha_2}(G) \ldots C^{(2)}_{\alpha_m}(G).$$

Using $C^{(2)}$, the cluster's centre of mass $\bar{\boldsymbol{r}}$ and number of sites s can be written

$$\bar{\boldsymbol{r}} = \frac{1}{N} \sum_\alpha \boldsymbol{r}^\alpha C^{(2)}_\alpha(G) \tag{2.10a}$$

$$s = \sum_\alpha C^{(2)}_\alpha(G). \tag{2.10b}$$

† This definition of S_d differs from that in [12] by a factor of two.

The shape of G is characterised by the radius of gyration tensor

$$R_{ij}^{(2)} = \frac{1}{s} \sum_{\alpha} (r_i^{\alpha} - \bar{r}_i)(r_j^{\alpha} - \bar{r}_j) C_{\alpha}^{(2)}(G). \tag{2.11}$$

We will find it computationally convenient to use instead the rescaled tensor $\boldsymbol{Q} = s^2 \boldsymbol{R}^{(2)}$, which can be rewritten

$$Q_{ij} = \tfrac{1}{2} \sum_{\alpha\beta} (r_i^{\alpha} - r_i^{\beta})(r_j^{\alpha} - r_j^{\beta}) C_{\alpha\beta}^{(3)}(G) \tag{2.12a}$$

$$= -\tfrac{1}{2} \partial_{q_i} \partial_{q_j}|_{\boldsymbol{q}=0} \sum_{\alpha\beta} \exp[i\boldsymbol{q} \cdot (\boldsymbol{r}^{\alpha} - \boldsymbol{r}^{\beta})] C_{\alpha\beta}^{(3)}(G) \tag{2.12b}$$

$$\equiv -\tfrac{1}{2} \partial_{q_i} \partial_{q_j}|_{\boldsymbol{q}=0} C^{(3)}(\boldsymbol{q}, -\boldsymbol{q}; G). \tag{2.12c}$$

Similarly, we can write

$$Q_{ij} Q_{kl} = (-\tfrac{1}{2})^2 \partial_i^1 \partial_j^1 \partial_k^2 \partial_l^2|_{\boldsymbol{q}^l=0} C^{(5)}(\boldsymbol{q}^1, -\boldsymbol{q}^1, \boldsymbol{q}^2, -\boldsymbol{q}^2; G) \tag{2.12d}$$

$$Q_{ij} Q_{kl} Q_{mn} = (-\tfrac{1}{2})^3 \partial_i^1 \partial_j^1 \partial_k^2 \partial_l^2 \partial_m^3 \partial_n^3|_{\boldsymbol{q}^l=0} C^{(7)}(\boldsymbol{q}^1, \ldots, -\boldsymbol{q}^3; G) \tag{2.12e}$$

where ∂_i^1 means $\partial/\partial q_i^1$. Using (2.12), we can compute Δ_d and S_d using only ensemble averages of Fourier transformed $C^{(m)}$. Let $\mathscr{C}^{(m)} \equiv \langle C^{(m)} \rangle$, where $\langle\,\rangle$ is an ensemble average. Then inserting (2.12) into (2.6) and into (2.8) yields

$$\Delta_d = \frac{d}{d-1} \frac{[(\nabla_1 \cdot \nabla_2)^2 - (1/d)\nabla_1^2 \nabla_2^2]_{\boldsymbol{q}^l=0} \mathscr{C}^{(5)}(\boldsymbol{q}^1, \ldots, -\boldsymbol{q}^2)}{[\nabla_1^2 \nabla_2^2]_{\boldsymbol{q}^l=0} \mathscr{C}^{(5)}(\boldsymbol{q}^1, \ldots, -\boldsymbol{q}^2)} \tag{2.13a}$$

$$S_d = \frac{d^2}{(d-1)(d-2)} \frac{\mathscr{O}(\nabla_1, \nabla_2, \nabla_3) \mathscr{C}^{(7)}(\boldsymbol{q}^1, \ldots, -\boldsymbol{q}^3)}{[\nabla_1^2 \nabla_2^2 \nabla_3^2]_{\boldsymbol{q}^l=0} \mathscr{C}^{(7)}(\boldsymbol{q}^1, \ldots, -\boldsymbol{q}^3)} \tag{2.13b}$$

$$\mathscr{O}(\nabla_1, \nabla_2, \nabla_3) \equiv [(\nabla_1 \cdot \nabla_2)(\nabla_2 \cdot \nabla_3)(\nabla_1 \cdot \nabla_3) - (1/d)(\nabla_1^2 (\nabla_2 \cdot \nabla_3)^2 + \text{permutations}) + (2/d^2) \nabla_1^2 \nabla_2^2 \nabla_3^2]_{\boldsymbol{q}^l=0}. \tag{2.13c}$$

We now proceed to evaluate (2.13) for bond percolation and lattice animals.

3. Bond percolation

In bond percolation, we average over all configurations of bonds on the lattice using a bond occupation probability p. Each configuration is thus weighted by $p^{N_b} q^{B-N_b}$, where B is the total number of bonds, N_b is the number of occupied bonds for this configuration, $0 \leqslant p \leqslant 1$ and $q = 1 - p$. It is worth noticing that this ensemble of lattice configurations leads to the same single-cluster statistics as would come from averaging over all connected clusters, if each cluster is weighted by $p^{N_b^c} q^{N_p^c}$, where N_b^c is the number of bonds in the cluster and N_p^c is the number of unoccupied bonds on the cluster's perimeter. N_b^c and N_p^c are illustrated in figure 1.

We will compute Δ and S at the percolation threshold p_c. Because the average number of sites in a cluster goes to infinity as $p \to p_{c-}$, we expect the large clusters to dominate our ensemble averages in this limit. Thus when we compute at p_c, we are actually computing the shapes of the asymptotically large clusters.

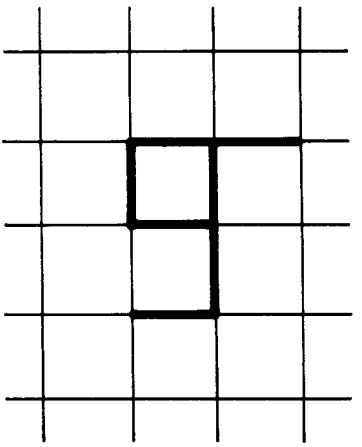

Figure 1. A cluster with $N_b^c = 7$ and $N_p^c = 13$. Its statistical weight is $p^7 q^{13}$.

As was first pointed out by Kasteleyn and Fortuin [15], bond percolation can be related to the Potts model. This relationship has been used by a number of investigators to explore properties of percolating systems [13]. Here we will generalise Stephen's mapping onto a Potts model [13] in order to compute $\langle \mathscr{C}^{(m)} \rangle$.

At each site α we put a spin λ_α which takes the values $\lambda = 1, \omega, \ldots, \omega^{n-1}$, where $\omega = \exp(2\pi i/n)$. In the $n \to 1$ limit the partition function

$$Z = A \operatorname{Tr}\left(\prod_{\text{bonds}} (1 + v\delta_{\lambda_\alpha \lambda_{\alpha'}}) \right) \tag{3.1}$$

with parameter values

$$v = p/q \qquad A = q^B$$

is that of bond percolation. To see this, multiply out the product over bonds and think of each $v\delta$ as an occupied bond. The multiplication results in a sum of traces of graphs $\mathscr{G}$, where a given $\mathscr{G}$ has the form

$$\mathscr{G} = A v_b^N \prod_{\langle \mathscr{G} \rangle} (\delta_{\lambda_\alpha \lambda_{\alpha'}}) \tag{3.2}$$

where $\Pi_{\langle \mathscr{G} \rangle}$ means a product over all occupied bonds of the graph $\mathscr{G}$. Upon taking the trace over spin configurations, we see that the δ allow one independent spin sum for each connected cluster in $\mathscr{G}$, so that

$$\operatorname{Tr} \mathscr{G} = A v^{N_b} n^{N_c} = q^{B - N_b} p^{N_b} n^{N_c} \tag{3.3}$$

where N_b is the number of bonds in $\mathscr{G}'$ and N_c is the number of connected clusters. When n is set to 1,

$$Z = \sum_{\text{graphs}} p^{N_b} q^{N - N_b} \tag{3.4}$$

which is the percolation partition function.

To obtain $\langle C^{(m+1)}_{\alpha_1 \ldots \alpha_m} \rangle$, we must restrict the sum in Z to the graphs in which the sites $\alpha_1, \ldots, \alpha_m$ are connected to the origin. Let $r_0, \ldots, r_m$ be a set of $m+1$ integers such

that $\Sigma r_i = 0 \bmod n$, but no subset of the r_i itself sums to 0 mod n. Then by explicit evaluation,

$$\mathrm{Tr}\left[\lambda_0^{r_0}\ldots\lambda_{\alpha_m}^{r_m}\prod_{\langle ij\rangle}\delta_{\lambda_{\alpha_i}\lambda_{\alpha_j}}\right]=\begin{cases}0 & \text{if } \alpha_1,\ldots,\alpha_m \text{ are not connected to the origin}\\ n^{N_c} & \text{otherwise.}\end{cases} \tag{3.5}$$

Accordingly,

$$\langle C^{(m+1)}_{\alpha_1\ldots\alpha_m}\rangle = \lim_{n\to 1}\frac{A\,\mathrm{Tr}[\lambda_0^{r_0}\ldots\lambda_{\alpha_m}^{r_m}\,\Pi_{\text{bonds}}(1+v\delta_{\lambda_\alpha\lambda_{\alpha'}})]}{Z}$$

$$= \lim_{n\to 1}\langle\lambda_0^{r_0}\ldots\lambda_{\alpha_m}^{r_m}\rangle_{\text{Potts}}. \tag{3.6}$$

This correlation function can be expressed in terms of a functional integral over a set of continuous fields $z_r(\alpha)$, $r=1,\ldots,n-1$, using the Hubbard–Stratonovich transformation [16]. Following Stephen [13] we find that near p_c, in the continuum limit

$$\mathscr{C}^{(m+1)}(\boldsymbol{q}^1,\ldots,\boldsymbol{q}^m)=\langle z_{r_0}(\boldsymbol{x}=0)z_{r_1}(\boldsymbol{q}_1)\ldots z_{r_m}(\boldsymbol{q}_m)\rangle \tag{3.7a}$$

$$=\int\frac{\mathrm{d}k}{(2\pi)^d}\langle z_{r_0}(\boldsymbol{k})z_{r_1}(\boldsymbol{q}_1)\ldots z_{r_m}(\boldsymbol{q}_m)\rangle \tag{3.7b}$$

where

$$\langle x\rangle=\lim_{n\to 1}\frac{\int\mathscr{D}z_r\,\mathrm{e}^{-\mathscr{H}}x}{\int\mathscr{D}z_r\,\mathrm{e}^{-\mathscr{H}}} \tag{3.7c}$$

and

$$\mathscr{H}=\int\mathrm{d}\boldsymbol{x}\left(\tfrac{1}{2}\,z_r^*(T_0-\nabla^2)z_r-\frac{w_0}{3!}\Delta(r_1+r_2+r_3)z_{r_1}z_{r_2}z_{r_3}\right). \tag{3.8}$$

In (3.8), summation convention is used on the spin indices, and all spin indices are to be taken as numbers mod n. With this convention, $z_r^*(\boldsymbol{x})=z_{-r}(\boldsymbol{x})$ and $\Delta(r)=1$ if $r=0$ and is 0 otherwise. If T_c is the critical temperature of the theory, then T_0-T_c is proportional to $p-p_c$. As is usual with such continuum models, an ultraviolet cut-off near $k=\Lambda$ is implicit, where Λ is of the order of the inverse lattice spacing. If we now let $G^{(m)}(\boldsymbol{q}_1,\ldots,\boldsymbol{q}_m)$ denote this theory's connected m-leg Green function at the spin index set $r_0,\ldots,r_m$, but with the global momentum-conserving δ function $(2\pi)^d\delta(\Sigma\,\boldsymbol{q}_i)$ factored off, then (3.7) implies that

$$\mathscr{C}^{(5)}(\boldsymbol{q}_1,-\boldsymbol{q}_1,\boldsymbol{q}_2,-\boldsymbol{q}_2)=G^{(5)}(\boldsymbol{0},\boldsymbol{q}_1,-\boldsymbol{q}_1,\boldsymbol{q}_2,-\boldsymbol{q}_2) \tag{3.9a}$$

$$\mathscr{C}^{(7)}(\boldsymbol{q}_1,\ldots,-\boldsymbol{q}_3)=G^{(7)}(\boldsymbol{0},\boldsymbol{q}_1,\ldots,-\boldsymbol{q}_3). \tag{3.9b}$$

We now can use the known scaling properties of the Green functions to compute Δ_d and S_d in the limit as $p\to p_c$. From a renormalisation group analysis, one finds that to leading order in the inverse cut-off a_0 [17]

$$G^{(m)}(\boldsymbol{q}^i,T_0-T_c,w_0)$$

$$\underset{T_0\to T_c}{\approx}A_p(m)(X_p[T_0-T_c])^{a_p(m)}G_R^{(m)}(\boldsymbol{q}^i(X_p[T_0-T_c])^{-b_p},t_R=\kappa,u_*;\kappa). \tag{3.10}$$

In (3.10), $A_p(m)$ and X_p are non-universal, $a_p(m)$ and b_p are critical exponents, and G_R is a Green function renormalised via minimal subtraction at the inverse length scale κ and computed at the matching point. At this matching point the renormalised

temperature t_R is set to κ and the renormalised coupling constant $u = w/(\kappa^{\varepsilon/2})$ has flowed to its fixed point value u_*. Combining (3.10) with (3.9) and substituting into our basic relation (2.13), we see that at p_c all of the non-universal factors cancel out of both Δ_d and S_d. In fact, to compute either Δ_d or S_d one simply must replace the $\mathscr{C}^{(m)}$ in (2.13) by renormalised Green functions evaluated at the matching point.

We first consider Δ_d. Following the above prescription, we explicitly find that

$$\Delta_d = \frac{d}{d-1} \frac{[(\nabla_1 \cdot \nabla_2)^2 - (1/d)\nabla_1^2\nabla_2^2]_{q^i=0} G_R^{(5)}(\mathbf{0}, \boldsymbol{q}^1, \ldots, -\boldsymbol{q}^2; *)}{[\nabla_1^2\nabla_2^2]_{q^i=0} G_R^{(5)}(\mathbf{0}, \boldsymbol{q}^1, \ldots, -\boldsymbol{q}^2; *)} \tag{3.11}$$

where $*$ means at the matching point. It is useful to expand $G_R^{(5)}$ first in a power series in the momenta $\boldsymbol{q}^1$ and $\boldsymbol{q}^2$. Because (3.11) is second order in both ∇_1 and in ∇_2, we will only need the coefficients of $(\boldsymbol{q}^1 \cdot \boldsymbol{q}^2)^2$ and $(q^1)^2(q^2)^2$ to calculate Δ_d. Upon differentiating, one sees that

$$((\nabla_1 \cdot \nabla_2)^2 - (1/d)\nabla_1^2\nabla_2^2) \begin{Bmatrix} (q^1)^2(q^2)^2 \\ (\boldsymbol{q}_1 \cdot \boldsymbol{q}_2)^2 \end{Bmatrix} = \begin{Bmatrix} 0 \\ 2(d-1)(d+2) \end{Bmatrix} \tag{3.12a}$$

$$(\nabla_1^2\nabla_2^2) \begin{Bmatrix} (q^1)^2(q^2)^2 \\ (\boldsymbol{q}_1 \cdot \boldsymbol{q}_2)^2 \end{Bmatrix} = \begin{Bmatrix} 4d^2 \\ 4d \end{Bmatrix}. \tag{3.12b}$$

Thus, using a $G_R^{(5)}$ of the form

$$G_R^{(5)}(\mathbf{0}, \boldsymbol{q}_1, \ldots, -\boldsymbol{q}_2; *) = \ldots + a(q^1)^2(q^2)^2 + b(\boldsymbol{q}_1 \cdot \boldsymbol{q}_2)^2 + \ldots \tag{3.13}$$

in (3.11) yields the result that

$$\Delta_d = \frac{d+2}{2(1+da/b)}. \tag{3.14}$$

We must now calculate a/b. In appendix 2 we renormalise (3.8) and show that $u_*^2 = 2\varepsilon/7$, where $\varepsilon = 6-d$. Thus, to $O(\varepsilon)$, $G_R^{(5)}$ is the sum of the graphs shown in figure 2. We expand these graphs in $\boldsymbol{q}_1$ and $\boldsymbol{q}_2$ before computing the loop integrals. This trivialises the loop integrals. Because all denominators now only involve the loop momentum, Feynman parameters are not needed. To keep proper track of the combinatorics and of all terms in the expansion in the $\boldsymbol{q}^i$, we performed the actual calculation using the symbolic manipulation package SMP†. Our resulting expansion for $G_R^{(5)}$ is shown in table 1. To get a final value for Δ_d, we expand (3.14) to $O(\varepsilon)$.

One should notice that Δ_d does not vanish when $d \geqslant 6$, even though the coupling constant u flows to $u_* = 0$. Because Δ_d depends upon the ratio a/b, a factor of u_*^3

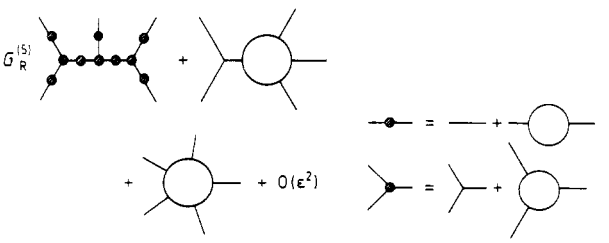

Figure 2. The graphs which contribute to $G_R^{(5)}$ to $O(\varepsilon)$. The first graph consists of the O(1) tree contribution, as well as all one-loop corrections to the tree's propagators and vertices.

† SMP version I.5.0., produced by Inference Corporation.

Table 1. The momentum expansions of $G^{(5)}$ and $G^{(7)}$ for percolation and animals. Both models have identical expansions of Green functions to O(1). We have lumped the three momentum combinations $(q^{i_1})^2(q^{i_2}\cdot q^{i_3})^2$ together because $\nabla_1^2\nabla_2^2\nabla_3^2$ does not distinguish between them.

$$G^{(5)}_{\text{percolation}} = \ldots + (168 + \tfrac{22\,636}{315}\varepsilon)(q^1\cdot q^2)^2 + (56 + \tfrac{9164}{315}\varepsilon)(q^1)^2(q^2)^2 + \ldots$$

$$G^{(5)}_{\text{animal}} = + \ldots (168 - \tfrac{3563}{30}\varepsilon)(q^1\cdot q^2)^2 + (56 - \tfrac{4837}{135}\varepsilon)(q^1)^2(q^2)^2 + \ldots$$

$$G^{(7)}_{\text{either}} = \ldots - \{36\,096(q^1\cdot q^2)(q^2\cdot q^3)(q^1\cdot q^3) + 76\,512(q^1)^2(q^2)^2(q^3)^2 + 78\,912[(q^1)^2(q^2\cdot q^3)^2 \text{ or permutations}]\}\ldots$$

cancels between the numerator and the denominator. All corrections to the tree approximation do, however, vanish at the matching point. Thus, when $d \geqslant 6$

$$\Delta_{d\geqslant 6} = (d+2)/(6d+2) \tag{3.15}$$

is exact. Because Δ_d has non-trivial d dependence above $d=6$, we have chosen to retain the exactly known dimension dependence resulting from q^i gradients. We expand to $O(\varepsilon)$ the asymptotically known ε dependence of a/b. Our resulting expression for Δ_d is listed in table 2.

Our treatment of S_d parallels that of Δ_d. Now, the relevant momentum combinations are $(q^1\cdot q^2)(q^2\cdot q^3)(q^1\cdot q^3)$, all permutations of $(q^1)^2(q_2\cdot q_3)^2$, and $(q^1)^2(q^2)^2(q^3)^2$. The operator $\mathcal{O}(\nabla_i)$ defined in (2.13) annihilates all momentum combinations except $(q^1\cdot q^2)(q^2\cdot q^3)(q^1\cdot q^3)$. Accordingly, to evaluate (2.13b) (with the substitution $\mathcal{G}^{(7)}\to G_R^{(7)}$) we need the identities

$$\mathcal{O}(\nabla_i)(q^1\cdot q^2)(q^2\cdot q^3)(q^1\cdot q^3) = (1/d)(d-1)(d-2)(d^2+6d+8) \tag{3.16a}$$

$$\nabla_1^2\nabla_2^2\nabla_3^2\begin{Bmatrix}(q^1\cdot q^2)(q^2\cdot q^3)(q^1\cdot q^3)\\ (q^1)^2(q_2\cdot q_3)^2\\ (q^1)^2(q^2)^2(q^3)^2\end{Bmatrix} = \begin{Bmatrix}8d\\ 8d^2\\ 8d^3\end{Bmatrix}. \tag{3.16b}$$

Table 2. Expansions of Δ_d to $O(\varepsilon)$ and S_d to O(1). Above each theory's critical dimension, the $\varepsilon = 0$ results are exact.

$$\Delta_d^{\text{percolation}} = \frac{2+d}{2+6d} + \frac{607}{4410}\frac{d(d+2)}{(1+3d)^2}\varepsilon_{\text{percolation}}$$

$$\Delta_d^{\text{animal}} = \frac{2+d}{2+6d} + \frac{29}{288}\frac{d(d+2)}{(1+3d)^2}\varepsilon_{\text{animal}}$$

$$\Delta_d^{\text{polymer}} = \frac{4+2d}{4+5d} + \frac{745}{3584}\frac{2d+4}{(5d+4)^2}\varepsilon_{\text{polymer}}$$

$$S_d^{\text{percolation or animal}} = \frac{47(d^2+6d+8)}{797d^2+822d+376} + O(\varepsilon)$$

$$S_d^{\text{polymer}} = \frac{8(d^2+6d+8)}{35d^2+84d+64} + O(\varepsilon)$$

$$\varepsilon_{\text{percolation}} = 6-d$$

$$\varepsilon_{\text{animal}} = 8-d$$

$$\varepsilon_{\text{polymer}} = 4-d$$

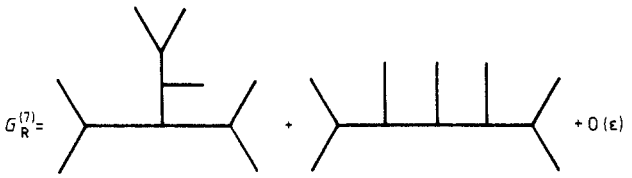

Figure 3. The graphs contributing to S_d to O(1).

We have computed S_d to leading order. The tree contributions to $G_R^{(7)}$ are shown in figure 3. We give the expansions of these graphs to second order in the q^i in table 1, and our resulting value for S_d in table 2.

4. Lattice animals

We now modify the above calculation to treat lattice animals. In this case we average over all single clusters, giving a weight of $p^{N_b}q^{N_p}h^{N_s}$ to each cluster containing N_b bonds, N_p perimeter bonds and N_s sites. A field theoretic representation of the animal ensemble has been developed by Harris and Lubensky [14]. We simplify their theory slightly and consider the partition function

$$Q = \mathrm{Tr}\left(\prod_{\langle \alpha\alpha' \rangle} (1 + v p_\alpha p_{\alpha'} \delta_{\lambda_\alpha \lambda_{\alpha'}}) \exp[-K_1(p_\alpha + p_{\alpha'} - p_\alpha p_{\alpha'})] \prod_{\text{sites}} (p_\alpha \, \mathrm{e}^{-H_1} + q_\alpha / n) \right) \tag{4.1a}$$

$$\equiv \mathrm{Tr}[\exp(-H_0(\{p_\alpha\}, \{q_\alpha\}))] \tag{4.1b}$$

where $p_\alpha = (0, 1)$ is a site occupation variable, $q_\alpha = 1 - p_\alpha$ and H_1 is an external field. Upon expanding the products and evaluating the trace, one finds that

$$Q = nN_s Z + \mathrm{O}(n^2) \tag{4.2}$$

where

$$Z = \sum_{\text{clusters}} (v \, \mathrm{e}^{K_1})^{N_b} (\mathrm{e}^{-K_1})^{N_p} (\mathrm{e}^{-H_1})^{N_s}. \tag{4.3}$$

The various animal partition functions are obtained by appropriate choices of v, K_1 and H_1. For instance, bond animals ($q = h = 1$) are obtained by choosing $K_1 = H_1 = 0$ and $v = p$.

To compute $\mathscr{C}^{(m)}$, we modify our percolation treatment and use the identity

$$\mathscr{C}^{(m+1)}_{\alpha_1 \ldots \alpha_m} = \lim_{n \to 0} \frac{(1/n) \, \mathrm{Tr}(p_0 \lambda_0^{r_0} p_{\alpha_1} \lambda_{\alpha_1}^{r_1} \ldots p_{\alpha_m} \lambda_{\alpha_m}^{r_m} \, \mathrm{e}^{-H_0})}{Z}. \tag{4.4}$$

After making a Hubbard-Stratonovich transformation [16], taking the continuum limit, dropping irrelevant interactions and rescaling we arrive at a field theoretic expression for $\mathscr{C}^{(m)}$:

$$\mathscr{C}^{(m+1)}(\boldsymbol{q}_1, \ldots, \boldsymbol{q}_m) = \mathscr{N} \lim_{n \to 0} n^{(m-1)/2} G^{(m+1)}\left(-\sum \boldsymbol{q}_i, \boldsymbol{q}_1, \ldots, \boldsymbol{q}_m \right). \tag{4.5}$$

In (4.5), $\mathcal{N}$ is a normalisation constant and $G^{(m+1)}$ is an $(m+1)$-leg Green function without the momentum conserving δ function, at spin indices $r_0, \ldots, r_m$, in the theory with free energy

$$\mathcal{H} = \int \mathrm{d}\boldsymbol{x} \left(\tfrac{1}{2} z_r^* (T_0 - \nabla^2) z_r + \tfrac{1}{2} n R z_0^2 - \frac{w_0}{3! \sqrt{n}} \Delta(r_1 + r_2 + r_3) z_{r_1} z_{r_2} z_{r_3} + \sqrt{n} H z_0 \right). \tag{4.6}$$

The spin sums in $\mathcal{H}$ now run from 0 to $n-1$, because the $z_{r\neq 0}$ fields from the percolation problem are now coupled to z_0. As before, $T_0 - T_c$ is proportional to $p - p_c$. For this calculation, we always work to leading order in n.

As is shown in appendix 3, $\mathcal{H}$ has upper critical dimension $d_c = 8$ because of the nRz_0^2 term. When R is non-zero, the theory's critical behaviour is dominated by a single lattice animal fixed point. Harris and Lubensky [14] show that the non-generic case of percolation ($q = (1-p)$ while $h = 1$) corresponds to the multicritical point $R = 0$. At this multicritical point, d_c reverts to six. The animal shape parameters we now compute are valid for the universality class of the animal fixed point. This class includes the case of bond animals.

The calculation is complicated by the fact that z_0 has a non-zero expectation value. Accordingly, to evaluate expressions like (4.5) in perturbation theory we must first shift z_0 to remove all tadpole graphs. For given H and T_0, let z_0 have expectation $\sqrt{n}Q$, defining the equation of state

$$(1/\sqrt{n})\langle z_0 \rangle = Q(H, T_0). \tag{4.7}$$

In the animal model H is fixed, while T_0 can vary. To investigate shapes at p_c, we will want to look at ratios of gradients of Green functions as T_0 approaches the critical temperature $T_c = T_c(H)$. Thus, we must investigate limits of the form

$$\lim_{T_0 \to T_c} \Big|_H \frac{G_1(T_0, H)}{G_2(T_0, H)} = \mathscr{L}_{12} \tag{4.8}$$

where the G_i are gradients of Green functions. Renormalisation groups are set up to directly treat theories at constant Q. For fixed Q, $H = H(Q, T_0)$ is set via the equation of state. By choosing to fix Q at the special value $Q = Q_c = Q(H, T_c(H))$, we can compute $\mathscr{L}_{12}$ using a theory at constant Q. Clearly,

$$\mathscr{L}_{12} = \lim_{T_0 \to T_c} \Big|_{Q = Q_c} \frac{G_1(T_0, Q_c)}{G_2(T_0, Q_c)}. \tag{4.9}$$

Just as in the percolation case, a renormalisation group analysis at constant Q shows that

$$G^{(m)}(\boldsymbol{q}^i, T_0 - T_c, w_0, R) \underset{T_0 \to T_c}{\approx} A_a(m)(X_a[T_0 - T_c])^{a_a(m)} G_R^{(m)}(\boldsymbol{q}^i (X_a[T_0 - T_c])^{-b_a}, t_R = \kappa, u_*; \kappa). \tag{4.10}$$

As for percolation, $A_a(m)$ and X_a are non-universal, while $a_a(m)$ and b_a are critical exponents. We now match by setting the renormalised temperature in the shifted theory, t_R, to the renormalisation scale κ. The true dimensionless renormalised coupling constant is $u = g/\kappa^\epsilon = w^2 R/\kappa^\epsilon$ which is set to its fixed point value at the matching point. We make no explicit reference to Q because it only enters our calculations by ensuring that the tadpole graphs vanish in the shifted theory.

Upon comparing (4.10) to (3.10), we see that to compute Δ_d and S_d for animals, we need the same coefficients in the momentum expansions of $G_R^{(5)}$ and $G_R^{(7)}$ as were needed for percolation. In appendix 3 we give a renormalisation group treatment of (4.6). Above d_c only tree graphs contribute to Δ_d and S_d, exactly as for percolation. But to tree order, the only way the Feynman rules for animals differ from those of percolation is in the bare propagator of the z_0 field. Because no subsum of the r_i indices of the external legs can sum to 0, there are no z_0 lines allowed. Thus, term by term, the tree contributions to $G_R^{(5)}$ and $G_R^{(7)}$ for animals are identical to those of the percolation model. Accordingly, above d_c animals and percolation clusters have the same shape parameters.

Below d_c there are corrections of $O(\varepsilon)$. We show in appendix 3 that these can be computed using a simple modification of the SMP code of our percolation calculation. The resulting expansion of $G_R^{(5)}$ is listed in table 1. Our value of Δ_d is in table 2.

5. Discussion

The results of our ε expansion are summarised in table 2. In tables 3 and 4, we have evaluated these formulae in dimensions $d = 2, 3, 6$ and ∞ for Δ_d, and in $d = 3, 6$ and ∞ for S_d. (Because $\mathrm{Tr}\,\hat{Q}^3 \equiv 0$ in $d = 2$, S_2 has no meaning.) We first notice that even in $d = 2$, where $\varepsilon_{\text{percolation}} = 4$ and $\varepsilon_{\text{animal}} = 6$, the corrections to mean-field theory are only about 30%. Thus, our ε expansion converges fast enough for a comparison of our results with those of Family *et al* [3] to be meaningful. We confirm that both percolation and animals have fairly anisotropic clusters. In both cases, Δ_2 is about 30% of its maximum value 1. This agrees qualitatively with the finding of Family *et al* [3] that A_2 is about 0.3-0.4, where $A_2 = 1$ implies spherical symmetry, but quantitatively our measure implies that the clusters are more symmetric than A_2 suggests. We do confirm that animals are a bit more anisotropic than percolation clusters, although our computed difference $\Delta_2^{\text{animal}} - \Delta_2^{\text{percolation}} \sim 0.091$ is a bit less than the difference $A_2^{\text{percolation}} - A_2^{\text{animal}} \sim 0.1$ found by Family *et al.* Considering that A_2 and S_2 are quite different measures of anisotropy and that we are comparing in a dimension where ε

Table 3. Numerical values for Δ_d, written in the form: mean field +(O(ε) correction).

	$\Delta_d^{\text{percolation}}$	Δ_d^{animal}	$\Delta_d^{\text{polymer}}$
$d = 2$	$0.286 + (0.088)$	$0.286 + (0.099)$	$0.577 + (0.016)$
$d = 3$	$0.250 + (0.062)$	$0.250 + (0.076)$	$0.526 + (0.006)$
$d = 6$	0.211	$0.211 + (0.027)$	0.471
$d = \infty$	$0.167 = \frac{1}{6}$	$0.167 = \frac{1}{6}$	$0.400 = \frac{2}{5}$

Table 4. Numerical values of S_d.

	S_d^{clusters}	S_d^{polymer}
$d = 3$	0.164	0.444
$d = 6$	0.111	0.350
$d = \infty$	$0.059 = \frac{47}{797}$	$0.229 = \frac{8}{35}$

is four for percolation and is six for animals, our agreement with Family *et al* seems reasonable.

Tables 2 and 3 show that $\Delta_d^{\text{animal}} \geqslant \Delta_d^{\text{percolation}}$ in all dimensions. This inequality can be understood by considering the relative weightings of a given cluster in the two models. For concreteness, we represent the animal universality class by bond animals. Then a cluster containing N_b bonds and whose perimeter contains N_p bonds has statistical weights W

$$W_{\text{animal}} = p^{N_b}$$

$$W_{\text{percolation}} = p^{N_b}(1-p)^{N_p}.$$

Compared to the animal problem, percolation has an effective surface tension. Clusters with larger perimeters are statistically suppressed. Accordingly, lattice animals should be more anisotropic than percolation clusters, unless almost all clusters of size N_b, for large N_b, have essentially the same N_p. This is precisely what one expects to happen above d_c, where the clusters are dominated by trees. Thus it is not surprising that percolation clusters and lattice animals have the same values of both Δ_d and S_d for $d \geqslant 8$.

In order to compare our results with Aronovitz and Nelson's results [12] for polymer shapes, we have converted their results to d-dimensional measures in appendix 4. We list the long-chain polymer values for Δ_d and S_d in tables 2-4, along with our results for clusters. It is clear that in all dimensions, polymers are both more anisotropic and more prolate than clusters are. Furthermore, there seems to be a general trend that models become more symmetric and less prolate as d is increased. Increased available phase space seems to favour symmetry.

Acknowledgments

JA would like to thank F Family for originally pointing out the percolation shape problem. While this research was in progress we benefited from conversions with Y Kantor, T C Lubensky, D R Nelson and S Milner. This work was supported by the National Science Foundation through grant DMR-85-14638 at Harvard and was partially supported by the National Science Foundation through grant DMR-84-05619 at Rutgers.

Appendix 1. Derivation of amplitude ratio inequalities

We first consider Δ_d and prove inequality (2.5). Suppose that the $\boldsymbol{Q}$ of a given cluster has average eigenvalue $\bar{\lambda}$. Recalling that $\hat{\boldsymbol{Q}} = \boldsymbol{Q} - \bar{\lambda}\mathbf{1}$ and that $\boldsymbol{Q}$ is positive definite, we see that the $\hat{\lambda}_i$ satisfy

$$\hat{\lambda}_i \geqslant -\bar{\lambda} \tag{A1.1a}$$

and

$$\sum_i \hat{\lambda}_i = 0. \tag{A1.1b}$$

Together, (A1.1a) and (A1.1b) define a $(d-1)$-dimensional simplex (hyper-tetrahedron) embedded in d space, centred at the origin ($\hat{\lambda}_i = 0$) with corners at coordinates

$\hat{\lambda}_{i_1} = (d-1)\bar{\lambda}$ and $\hat{\lambda}_{j\neq i_1} = -\bar{\lambda}$. This embedding is illustrated for the drawable case of $d=3$ in figure 4(a). The simplex appropriate to $d=4$ is shown in figure 4(b). Let a particular set of $\hat{\lambda}_i$ lie at the vector $\boldsymbol{v} = (\hat{\lambda}_1, \ldots, \hat{\lambda}_d)$. Then

$$\mathrm{Tr}\,\hat{\boldsymbol{Q}}^2 = \sum_i \hat{\lambda}_i^2 = \boldsymbol{v}\cdot\boldsymbol{v}. \tag{A1.2}$$

We see that $\mathrm{Tr}\,\hat{\boldsymbol{Q}}^2$ is maximised when $\boldsymbol{v}$ is as large as it can be. This occurs at the simplex's corners. The minimal value $\mathrm{Tr}\,\hat{\boldsymbol{Q}}^2 = 0$ is achieved at the centre ($\boldsymbol{v}=\boldsymbol{0}$). Thus,

$$0 \leqslant \mathrm{Tr}\,\hat{\boldsymbol{Q}}^2 \leqslant [(d-1)\bar{\lambda}]^2 + (d-1)\bar{\lambda}^2 = (d-1)d\bar{\lambda}^2 = [(d-1)/d](\mathrm{Tr}\,\boldsymbol{Q})^2 \tag{A1.3}$$

and (2.5) is proved.

The proof of (2.7) is more involved. We first notice that if $\boldsymbol{v}_1 = \alpha\boldsymbol{v}_2$, then $\mathrm{Tr}\,\hat{\boldsymbol{Q}}_1^3 = \alpha^3\,\mathrm{Tr}\,\hat{\boldsymbol{Q}}_2^3$. Accordingly, $f(\hat{\boldsymbol{Q}}) = \mathrm{Tr}\,\hat{\boldsymbol{Q}}^3$ must reach its extremal values on the simplex's boundary. As a step towards finding these extrema we first treat f on the set

$$\mathcal{S} = \{\boldsymbol{v} | \boldsymbol{v}^2 = R^2\} \cap \left\{\boldsymbol{v} \middle| \sum \hat{\lambda}_i = 0\right\}. \tag{A1.4}$$

The construction of $\mathcal{S}$ in three dimensions is shown in figure 5. Using Lagrange

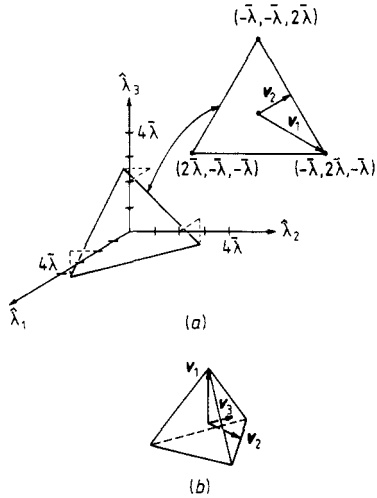

Figure 4. The cases $d=3$ and $d=4$. (a) The 2-simplex embedded in three space; (b) the 3-simplex. The vectors $\boldsymbol{v}^m$ are also illustrated.

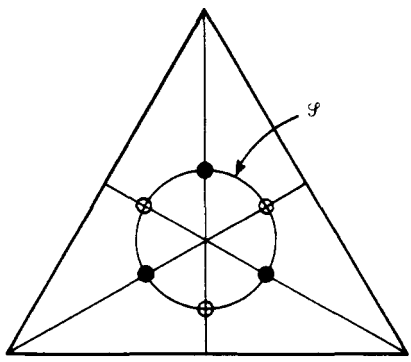

Figure 5. $\mathcal{S}$ is shown for the case $d=3$. The open circles are the minimising extrema $\boldsymbol{v}^2$, while the full circles are the maximising extrema $\boldsymbol{v}^1$.

multipliers, one can easily show that the components $\hat{\lambda}_i^e$ of a given extremal vector $\boldsymbol{v}^e$ can have only two values. Because $\Sigma_i \hat{\lambda}_i^e = 0$, the only possible extrema occur at the vectors $\boldsymbol{v}^m$ such that m of the components of $\boldsymbol{v}^m$ have the value $(d-m)|x|/m$, while the other $(d-m)$ components are $-|x|$. $\boldsymbol{v}^m$ must also satisfy $(\boldsymbol{v}^m)^2 = R^2$, which implies that

$$x^2 = \frac{mR^2}{d(d-m)}. \tag{A1.5}$$

For convenience, we choose $R^2 = d$. We now see that

$$\sum \hat{\lambda}_i^3 = \frac{d(d/m-2)}{(d/m-1)^{1/2}} \tag{A1.6}$$

is a strictly decreasing function of m for the case of interest, $m < d$. Thus, $\Sigma \hat{\lambda}_i^3$ is minimised on $\mathcal{S}$ at $\boldsymbol{v}^{(d-1)}$ and is maximised at $\boldsymbol{v}^1$.

The $\boldsymbol{v}^{(d-1)}$ point to the centres of the faces of the simplex, while the $\boldsymbol{v}^1$ point to its corners. The face centres are the points on the simplex's boundary which are closest to the origin, while the corners are furthest away. Thus the amount of scaling necessary to project a point from $\mathcal{S}$ onto the simplex is smallest at the $\boldsymbol{v}^{(d-1)}$ and is greatest for the $\boldsymbol{v}^1$. Accordingly, $\Sigma \hat{\lambda}_i^3$ is minimised on the simplex at the face centres $\boldsymbol{v}^{\min}$ and is maximised at the simplex's corners. $\boldsymbol{v}^{\min}$ has $d-1$ components with the value $\bar{\lambda}/(d-1)$, and one component $-\bar{\lambda}$. Thus,

$$-\bar{\lambda}^3 + (d-1)\frac{1}{(d-1)^3}\bar{\lambda}^3 \leqslant \sum \hat{\lambda}_i^3 \leqslant (d-1)^3\bar{\lambda}^3 - (d-1)\bar{\lambda}^3 \tag{A1.7}$$

or, in terms of traces,

$$-\frac{(\mathrm{Tr}\,\boldsymbol{Q})^3}{(d-1)^3} \leqslant \frac{d^2}{(d-1)(d-2)}\,\mathrm{Tr}\,\hat{\boldsymbol{Q}}^3 \leqslant (\mathrm{Tr}\,\boldsymbol{Q})^3 \tag{A1.8}$$

and (2.7) is proved.

Our interpretation of $\mathrm{Tr}\,\hat{\boldsymbol{Q}}^3$ as a measure of a generalised version of oblateness against prolateness follows from the observation that for the critical points $\boldsymbol{v}^m$, the sign of $\mathrm{Tr}\,\hat{\boldsymbol{Q}}^3$ is positive when there are less large eigenvalues than small ones. This qualitatively indicates the trend in the sign of $\mathrm{Tr}\,\hat{\boldsymbol{Q}}^3$.

Appendix 2. Renormalisation of the Potts model

In this appendix, we renormalise the Potts model (3.8). Our treatment is similar to that of Amit [18] who treats a slightly different representation of this model. We first define the dimensionless bare coupling constant u_0 by

$$w_0 = u_0 \kappa^{\varepsilon/2}. \tag{A2.1}$$

We then use minimal subtraction to fix u_0 and the renormalisation functions Z_ϕ and $\bar{Z}_{\phi^2}$ by demanding, in the critical theory ($T_0 = T_c$), that the renormalised vertex functions

$$\Gamma_R^{(2)} = Z_\phi \Gamma^{(2)} \tag{A2.2a}$$

$$\Gamma_R^{(3)} = Z_\phi^{3/2}\Gamma^{(3)} \tag{A2.2b}$$

$$\Gamma_R^{(2,1)} = \bar{Z}_{\phi^2}\Gamma^{(2,1)} \tag{A2.2c}$$

are finite. To $O(u^2)$, the relevant graphs are shown in figure 6.

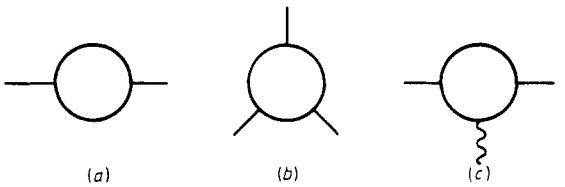

Figure 6. The graphs which renormalise (*a*) $\Gamma^{(2)}$, (*b*) $\Gamma^{(3)}$ and (*c*) $\Gamma^{(2,1)}$.

We find that to $O(u^2)$

$$Z_\phi = 1 + [(2-n)/6\varepsilon]u^2 \tag{A2.3a}$$

$$\bar{Z}_{\phi^2} = 1 + [(2-n)/\varepsilon]u^2 \tag{A2.3b}$$

$$u_0 = u\{1 + [(10-3n)/4\varepsilon]u^2\}. \tag{A2.3c}$$

In the standard way [17], these relations lead to the β function

$$\beta = -\tfrac{1}{2}\varepsilon(\partial \ln u_0/\partial u)^{-1} = -\tfrac{1}{2}u[\varepsilon - \tfrac{1}{2}(10-3n)u^2] \tag{A2.4}$$

and to the expected exponents (in the $n \to 1$ limit),

$$\eta_{\text{Potts}} = -\tfrac{1}{21}\varepsilon \tag{A2.5a}$$

$$\nu^{-1}_{\text{Potts}} = 2 - \tfrac{5}{21}\varepsilon. \tag{A2.5b}$$

The fixed point coupling constant at $n = 1$ is

$$u_*^2 = \tfrac{2}{7}\varepsilon. \tag{A2.6}$$

At finite temperature, renormalised Green functions are computed using the formula

$$G_R^{(m)}(\boldsymbol{q}^i, t_r, u, \kappa) = Z_\phi^{-(m/2)} G^{(m)}(\boldsymbol{q}^i, (T_0 - T_c) = t_r \bar{Z}_{\phi^2}/Z_\phi, w_0). \tag{A2.7}$$

Appendix 3. Renormalisation of the lattice animal model

Consider the shifted theory defined by (4.6). At bare shifted temperature T_0^Q and to leading order in n, the z_r fields have the bare propagators

$$g_r(\boldsymbol{q}) = \frac{1}{q^2 + T_0^Q} - \frac{nR\delta_{[r0]}}{(q^2 + T_0^Q)^2} \tag{A3.1a}$$

$$\equiv g(q) - nR\delta_{r_0} g^2(q). \tag{A3.1b}$$

To see how the z_0 field modifies perturbation theory, consider expanding $\Gamma^{(2)}_{r\neq 0}(q)$ to one-loop order. The relevant graphs are shown in figure 7. Writing them out explicitly

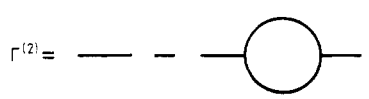

Figure 7. The expansion of $\Gamma^{(2)}_{r\neq 0}(q)$ to one-loop order.

and discarding terms which vanish when $n \to 0$ we see that

$$\Gamma^{(2)}_{r\neq 0}(q) = g(q) - \frac{w_0^2}{2n}\sum_{\bar{r}} \int \frac{d\boldsymbol{k}}{(2\pi)^d}(g(k) - nR\delta_{[0\bar{r}]}g^2(k)) \times [g(|\boldsymbol{k}+\boldsymbol{q}|) - nR\delta_{[0(r+\bar{r})]}g^2(|\boldsymbol{k}+\boldsymbol{q}|)] \tag{A3.2a}$$

$$= g(q) - \frac{w_0^2}{2}\int \frac{d\boldsymbol{k}}{(2\pi)^d}[g(k)g(|\boldsymbol{k}+\boldsymbol{q}|) - 2Rg^2(k)g(|\boldsymbol{k}+\boldsymbol{q}|)]. \tag{A3.2b}$$

We now consider the $nRz_0^2/2$ term in the action to be a new vertex, rather then a part of the bare propagator. Viewed this way, (A3.2*b*) has two types of one-loop corrections to $\Gamma^{(2)}$: the first term, in which no nRz_0^2 vertex is inserted and where the sum over internal spin components gives a factor of n, and the second term, in which an nR is explicitly inserted and where there is no spin sum.

This pattern of contributions to leading order in n is generally true. Because the nR insertions force an extra propagator into each loop, they are more infrared divergent than the other terms. This raises the critical dimension of the theory to eight. Near $d = 8$ the terms without an nR insertion are irrelevant to the inferred behaviour of the theory. Unfortunately, above $d = 6$ these irrelevant terms are non-renormalisable in the ultraviolet. To get around this technical problem, we define a renormalised perturbation theory which, when cut off, reproduces the leading inferred divergences near $d = 8$. To do this, we take the limit $w_0^2 \to 0$ while keeping $w_0^2 R$ fixed. Within this scheme, to leading order in n

$$\Gamma_r^{(2)} = g(q) - \omega_0^2 R \int \frac{d\boldsymbol{k}}{(2\pi)^d} g^2(k)g(|\boldsymbol{k}+\boldsymbol{q}|) + O(n^2). \tag{A3.3}$$

The pure w_0^2 term has been dropped.

By its construction, this new theory has the same divergence structure as the Potts model, except that now we expand about $d_c = 8$ rather than $d_c = 6$. The dimensionless coupling constant is now

$$u \equiv g/\kappa^\varepsilon = w^2 R/\kappa^\varepsilon. \tag{A3.4}$$

As in appendix 2, we fix u_0 and the renormalisation functions using minimal subtraction. We again demand that (A2.2) are finite in the critical theory and add the additional renormalisation condition that $R_0 = R$. We find that

$$Z_\phi = 1 + (1/2\varepsilon)u \tag{A3.5a}$$

$$\bar{Z}_{\phi^2} = 1 + (3/\varepsilon)u \tag{A3.5b}$$

$$u_0 = u[1 + (9/2\varepsilon)u] \tag{A3.5c}$$

$$w_0 = w[1 + (9/4\varepsilon)u] \tag{A3.5d}$$

so that

$$\beta(u) = -\varepsilon(\partial \ln u_0/\partial u)^{-1} = -u(\varepsilon - \tfrac{9}{2}u) \tag{A3.6}$$

and

$$u_* = \tfrac{2}{9}\varepsilon. \tag{A3.7}$$

These relations lead to the critical exponents

$$\eta = -\tfrac{1}{9}\varepsilon \tag{A3.8a}$$

$$\nu = \tfrac{1}{2} + \tfrac{5}{36}\varepsilon \tag{A3.8b}$$

which agree with the values Lubensky and Isaacson [2] have calculated for this model.

It is useful to notice that computing a one-loop graph in this theory is equivalent to computing the graph using the percolation Feynman rules with all spin sums suppressed, and then differentiating once with respect to T_0 and replacing w_0^2 with g_0. This rule is explicitly verified by our above computation of $\Gamma^{(2)}$:

$$-w_0^2 R \int \frac{\mathrm{d}\boldsymbol{k}}{(2\pi)^d}\, g^2(k) g(|\boldsymbol{k}+\boldsymbol{q}|) = R \frac{\mathrm{d}}{\mathrm{d}T_0^Q}\left(\frac{w_0^2}{2}\int \frac{\mathrm{d}\boldsymbol{k}}{(2\pi)^d}\, g(k) g(|\boldsymbol{k}+\boldsymbol{q}|)\right). \tag{A3.9}$$

To prove the rule, we first notice that changing the $nRz_0^2/2$ term in the action to $nRz_r z_{-r}$ (for $r \neq 0$ not summed over) does not change the value of any one-loop graph which we need for Δ_d or S_d. Thus a one-loop graph which has the value G will have the new value $G_{\text{new}} = nG$ in the new theory where $nRz_0^2/2$ is replaced by $\Sigma\, nRz_r z_{-r}/2$. This replacement can be absorbed into a temperature shift, $T_0^Q \to T_0^Q + nR$. This shift gives back the percolation Feynman rules, except that spin sums now carry a factor of n which cancels the $1/n$ in $G = G_{\text{new}}/n$. Our derivative rule follows from expanding G_{new} to leading order in n and setting w_0^2 to 0 while holding Rw_0^2 constant.

The rule allows us to compute the $O(\varepsilon)$ corrections to Δ_d for animals using the same graphs and combinatorics as were used for percolation. The T_0^Q derivative can be considered to be a change in the rules for evaluating one-loop integrals. Thus, we can compute the $O(\varepsilon)$ corrections to Δ_d for animals using essentially the same SMP code as was used for percolation.

Appendix 4. Conversion of polymer shape results

In this appendix, we adapt Aronovitz and Nelson's results on polymer shapes to give formulae in a form easily comparable to ours. To compute Δ_d and S_d for polymers, one makes the replacements

$$G_{\mathrm{R}}^{(5)}(\mathbf{0}, \boldsymbol{q}^1, \ldots, -\boldsymbol{q}^2; *) \to G_{\mathrm{R}}^{(2,4)}(\mathbf{0}, \mathbf{0}; \boldsymbol{q}^1, \ldots, -\boldsymbol{q}^2; *) \tag{A4.1a}$$

$$G_{\mathrm{R}}^{(7)}(\mathbf{0}, \boldsymbol{q}^1, \ldots, -\boldsymbol{q}^3; *) \to G_{\mathrm{R}}^{(2,6)}(\mathbf{0}, \mathbf{0}; \boldsymbol{q}^1, \ldots, -\boldsymbol{q}^3; *) \tag{A4.1b}$$

where $G_{\mathrm{R}}^{(2,m)}(*)$ is a propagator with M momentum insertions in the theory with free energy functional

$$\mathscr{H} = \int \mathrm{d}\boldsymbol{x}\, \tfrac{1}{2}\boldsymbol{S}\cdot(-\nabla^2 + T)\boldsymbol{S} + (\lambda/4!)(\boldsymbol{S})^4. \tag{A4.2}$$

In (A4.2), $\boldsymbol{S}$ is an n-component field, the limit $n \to 0$ is to be taken on all Green functions and the matching point is at $t_{\mathrm{R}} = \kappa$ and $u_* = 3\varepsilon/4$.

To compute Δ_d we need

$$G_{\mathrm{R}}^{(2,4)} = \ldots + a(q^1)^2(q^2)^2 + b(\boldsymbol{q}^1 \cdot \boldsymbol{q}^2) + \ldots. \tag{A4.3}$$

Aronovitz and Nelson report that

$$(\partial_x^1)^2(\partial_x^2)^2|_{\boldsymbol{q}^i=0}\, G_{\mathrm{R}}^{(2,4)} = 4(a+b) = 576 + \tfrac{1007}{5}\varepsilon \tag{A4.4a}$$

$$(\partial_x^1)^2(\partial_y^2)^2|_{\boldsymbol{q}^i=0}\, G_{\mathrm{R}}^{(2,4)} = 4a = 320 + 109\varepsilon \tag{A4.4b}$$

$$(\partial_x^1\partial_y^1)(\partial_x^2\partial_y^1)|_{\boldsymbol{q}^i=0}\, G_{\mathrm{R}}^{(2,4)} = 2b = 120 + \tfrac{231}{5}\varepsilon \tag{A4.4c}$$

so that

$$a = 80 + \tfrac{109}{4}\varepsilon \tag{A4.5a}$$

$$b = 64 + \tfrac{231}{10}\varepsilon \tag{A4.5b}$$

and from (3.15)

$$\Delta_d^{\text{polymer}} = \frac{d+2}{2(1+da/b)} = \frac{2+d}{2(1+5d/4)} + \frac{745}{7168}\frac{2+d}{(1+5d/4)^2}\varepsilon. \tag{A4.6}$$

To compute S_d, we directly computed that

$$G_{\mathrm{R}}^{(2,6)}(*) = \ldots - \{512(\boldsymbol{q}^1\cdot\boldsymbol{q}^2)(\boldsymbol{q}^2\cdot\boldsymbol{q}^3)(\boldsymbol{q}^1\cdot\boldsymbol{q}^3) + 280(q^1)^2(q^2)^2(q^3)^2 + 672[(q^1)^2(\boldsymbol{q}^2\cdot\boldsymbol{q}^3)^2 \text{ or permutations}]\} + \ldots \tag{A4.7}$$

which implies that

$$S_d^{\text{polymer}} = \frac{8(d^2+6d+8)}{35d^2+84d+64}. \tag{A4.8}$$

References

[1] Essam J W 1972 *Phase Transitions and Critical Phenomena* vol 2, ed C Domb and M S Green (New York: Academic) p 197
Stauffer D 1979 *Phys. Rep.* **54** 1
[2] Lubensky T C and Isaacson J 1979 *Phys. Rev.* A **20** 2130
[3] Family F, Vicsek T and Meakin P 1985 *Phys. Rev. Lett.* **55** 641
[4] Šolc K and Stockmayer W H 1971 *J. Chem. Phys.* **54** 2756
[5] Šolc K 1971 *J. Chem. Phys.* **55** 335
[6] Mazur J C, Guttman M and McCrackin F L 1973 *Macromol.* **6** 873
[7] Rubin R and Mazur J 1975 *J. Chem. Phys.* **63** 5362
[8] Rubin R and Mazur J 1977 *Macromol.* **10** 139
[9] Kranbuehl D E and Verdier P H 1977 *J. Chem. Phys.* **67** 361
[10] Rudnick J and Gaspari G 1986 *J. Phys. A: Math. Gen.* **19** L191
[11] Rudnick J, Beldjenna A and Gaspari G 1987 *J. Phys. A: Math. Gen.* **20** 971
[12] Aronovitz J A and Nelson D R 1987 *J. Physique* **47** 1445
[13] Harris A B, Lubensky T C, Holcomb W K and Dasgupta C 1975 *Phys. Rev. Lett.* **35** 327
Stephen M J 1977 *Phys. Rev.* B **15** 5674
[14] Harris A B and Lubensky T C 1981 *Phys. Rev.* B **23** 3591
[15] Kasteleyn P W and Fortuin C M 1969 *J. Phys. Soc. Japan Suppl.* **26** 11
[16] Hubbard J 1955 *Phys. Rev. Lett.* **3** 77
Stratonovich R L 1958 *Sov. Phys.-Dokl.* **2** 416
[17] Amit D J 1978 *Field Theory, the Renormalization Group, and Critical Phenomena* (New York: McGraw-Hill)
[18] Amit D J 1976 *J. Phys. A: Math. Gen.* **9** 1441